European Polymer Journal 44 (2008) 1673–1685

Contents lists available at ScienceDirect

European Polymer Journal

journal homepage: www.elsevier.com/locate/europolj

Macromolecular Nanotechnology

Chlorinated polyethylene nanocomposites using PCL/clay nanohybrid masterbatches

Samira Benali [a,*], Sophie Peeterbroeck [a], Patrick Brocorens [b], Fabien Monteverde [c], Leïla Bonnaud [c], Michaël Alexandre [d], Roberto Lazzaroni [b,c], Philippe Dubois [a,c,*]

[a] Laboratory of Polymeric and Composite Materials (LPCM), Center of Innovation and Research in Materials and Polymers (CIRMAP), University of Mons-Hainaut, Académie Universitaire Wallonie-Bruxelles, Place du Parc 20, B-7000 Mons, Belgium
[b] Laboratory for Chemistry of Novel Materials, Center of Innovation and Research in Materials and Polymers (CIRMAP), University of Mons-Hainaut, Académie Universitaire Wallonie-Bruxelles, Place du Parc 20, B-7000 Mons, Belgium
[c] Materia Nova asbl, Parc Initialis, Av. Nicolas Copernic 1, B-7000 Mons, Belgium
[d] Center for Education and Research on Macromolecules, Chemistry Institute (B6a), University of Liège, B-4000 Liège, Belgium

ARTICLE INFO

Article history:
Received 11 September 2007
Received in revised form 20 February 2008
Accepted 11 March 2008
Available online 31 March 2008

Keywords:
Chlorinated polyethylene
Poly(ε-caprolactone)/clay nanohybrid
Organophilic montmorillonite
Melt intercalation
In situ polymerization
Masterbatch

ABSTRACT

Exfoliated nanocomposites were prepared by dispersion of poly(ε-caprolactone) (PCL) grafted montmorillonite nanohybrids used as masterbatches in chlorinated polyethylene (CPE). The PCL-grafted clay nanohybrids with high inorganic content were synthesized by *in situ* intercalative polymerization of ε-caprolactone between silicate layers organo-modified by alkylammonium cations bearing two hydroxyl functions. The polymerization was initiated by tin alcoholate species derived from the exchange reaction of tin(II) bis(2-ethylhexanoate) with the hydroxyl groups borne by the ammonium cations that organo-modified the clay. These highly filled PCL nanocomposites (25 wt% in inorganics) were dispersed as masterbatches in commercial chlorinated polyethylene by melt blending. CPE-based nanocomposites containing 3–5 wt% of inorganics have been prepared. The formation of exfoliated nanocomposites was assessed both by wide-angle X-ray diffraction and transmission electron microscopy. The thermal and thermo-mechanical properties were studied as a function of the filler content, by differential scanning calorimetry and dynamic mechanical analysis, respectively. The mechanical properties were also assessed by tensile tests. The Young's modulus of CPE is increased by a decade when a PCL-grafted clay masterbatch is exfoliated to reach 5 wt% of clay in the resulting nanocomposite. The influence of PCL-grafting on the properties of these nanocomposites was investigated by comparison with materials obtained with ungrafted-PCL.

1. Introduction

Polymer nanocomposites constitute a class of polymers reinforced with a small amount (typically less than 10% in weight) of particles with nanometric size. Over the past years [1–4], the scientific community has largely focused on the polymer-clay nanocomposites owing to the improved properties that can be obtained with such nano-dimensional materials. Among other improvements, tensile, thermal and flame retardancy properties are increased [1–5] while gas transport properties can be significantly decreased [6,7]. For this purpose, layered silicate minerals, such as sodium montmorillonite (MMT) organo-modified by adequately chosen alkylammonium cations, are extensively used. Indeed, this crystalline 2:1 layered clay mineral is environmentally friendly, readily available in large quantities and its intercalation chemistry has been

* Corresponding authors. Address: Laboratory of Polymeric and Composite Materials (LPCM), Center of Innovation and Research in Materials and Polymers (CIRMAP), University of Mons-Hainaut, Académie Universitaire Wallonie-Bruxelles, Place du Parc 20, B-7000 Mons, Belgium (P. Dubois). Tel.: +32 65 37 33 70; fax: +32 65 37 34 84.
E-mail addresses: samira.benali@umh.ac.be (S. Benali), philippe.dubois@umh.ac.be (P. Dubois).

0014-3057/$ - see front matter © 2008 Elsevier Ltd. All rights reserved.
doi:10.1016/j.eurpolymj.2008.03.020

well studied [8]. The reinforcing action of these organo-modified clays has been investigated in a large variety of polymer matrices including polyolefins [9–12], polyesters [13–16], etc.

Depending on the nano-scale dispersion of the layered silicate, the whole spectrum of structure ranging from intercalated to exfoliated nanocomposites can be observed [1,17]. However, only delaminated structures lead to the complete and uniform dispersion of the individual silicate layers in a continuous polymer matrix and optimization of the mechanical and barrier properties.

Chlorinated polyethylene (CPE), obtained by free-radical substitution of hydrogen atoms of polyethylene by chlorine [18], is a polymer mainly used in thermoplastic processes, to modify the impact properties of rigid poly(vinyl chloride) (PVC) for applications such as vinyl siding and window profiles, but also in film and automotive applications, cable jackets and industrial sheets, because of its excellent resistance to ozone, UV radiation and oil [19]. However, the loss of hydrochloric acid, at temperatures higher than 150 °C, represents a major drawback [20] which limits the use of CPE. The most common way to overcome such drawback is to add stabilizers (hindered phenols, magnesium oxide, epoxidized soybean oil etc.). Furthermore, talc is commonly used as an anti-agglomeration additive in the case of suspension chlorination of PE [21].

The preparation of CPE/clay nanocomposites offers a novel approach to obtain new materials with improved mechanical and fire resistance properties, but only a few studies have been reported so far. Kim and White [22] prepared CPE/layered silicate nanocomposites with natural and organo-treated MMT by melt blending and discussed the mechanical properties enhancement with organoclays. These authors suggest that the CPE polymer chains largely intercalate the clay layers of their organoclay (Cloisite®30B). However, a close examination of the WAXD pattern points out a diffraction peak at $2\theta \approx 6°$, characteristic for the degradation of the intercalated ammoniums, as described later on in other publications [23,24].

In order to improve the nanocomposite structure (exfoliation) and its related performances, it has been suggested to use masterbatches where a high clay content is premixed/dispersed in a polymer known to behave as a compatibilizer for the selected matrix [25,26]. Owing to its known miscibility with CPE [27], poly(ε-caprolactone) (PCL) can be considered as a good compatibilizing agent.

Highly destructurated and even exfoliated nanocomposites based on PCL can be prepared by *in situ* polymerization of ε-caprolactone (CL) in the presence of montmorillonite modified by alkylammonium cations containing a carboxylic acid [28] or hydroxyl end-group(s) [29,30]. Therefore, largely exfoliated CPE/clay nanocomposites might be prepared by combining the *in situ* intercalative polymerization of CL within the organoclay to prepare highly destructurated masterbatches, followed by melt processing of this masterbatch with the CPE matrix.

Such a masterbatch strategy has been used with PVC nanocomposites by Lepoittevin et al. [17] with interesting results. Grafted-PCL masterbatches with high clay content (32 wt%) were obtained *by in situ* intercalative polymerization of CL in the presence of $Bu_2Sn(MeO)_2$ catalyst, then dispersed in a commercial PVC matrix to prepare largely exfoliated PVC/clay nanocomposites with improved mechanical properties. The conditions necessary to control all the molecular parameters of the grafted polyester chains, i.e., control over the grafting efficiency, grafting density, length of the grafted polyester chains, have been extensively studied by Lepoittevin et al. [14,15].

Based on those studies, we propose a two-step preparation of CPE-based nanocomposites. In a first step, the organomodified silicate layers are delaminated by the catalyzed polymerization of CL directly initiated from hydroxyl groups borne by the exchanged ammonium cations, in order to prepare masterbatches with a filler content of about 25 wt%. Then, the resulting polyester-grafted organoclay masterbatches are dispersed in a commercial CPE matrix by melt blending for reaching 3 and 5 wt% of clay (and thus 8.4 and 13.7 wt% of PCL, respectively). The morphological, thermal and mechanical properties of the resulting materials have been investigated. To assess the role of PCL-grafting and of the different components of the nanocomposites (CPE, clay, and PCL) on the materials properties, composites of lower complexity were also prepared and analyzed: CPE/PCL blends, CPE/clay blends, and CPE nanocomposites obtained from a non-grafted-PCL/clay masterbatch.

2. Experimental part

2.1. Materials

ε-Caprolactone (CL, Fluka) was dried over CaH_2 and distilled under reduced pressure prior to use. Tin (II) bis(2-ethylhexanoate), also known as tin(octoate) ($Sn(Oct)_2$), was purchased from Fluka, diluted with dried toluene and stored under nitrogen atmosphere.

Commercial CPE, Tyrin®3611P (36 wt% chlorine), obtained from a chlorination process of linear high-density polyethylene, was supplied by Dupont-Dow Elastomers. The supplier notes the presence of talc in the CPE matrix (<7 wt%). CAPA®2402, a PCL oligomer (Mn = 4000 g mol^{-1}) was obtained from Solvay Interox. Cloisite®30B (CL30B), a montmorillonite organomodified by 23.4 wt% of methyl bis(2-hydroxyethyl)tallowalkyl ammonium cations was supplied by Southern Clay Products.

2.2. Preparation of poly(ε-caprolactone)/clay masterbatches

Poly(ε-caprolactone) (PCL) has been grafted on the organoclay surface by ring-opening polymerization of ε-caprolactone (CL) in the presence of $Sn(Oct)_2$ according to a 'coordination-insertion' mechanism in appropriate conditions [14].

Before polymerization, the organo-modified montmorillonite (CL30B) (5.25 g) was dried under vacuum (10^{-2} mm Hg) at 70 °C overnight in a glass reactor equipped with a magnetic stirrer. A toluene solution of $Sn(Oct)_2$ (7 mL, 3.5 10^{-4} mol) was then added to the clay under nitrogen flow. A given amount of ε-caprolactone (11 mL, 0.09 mol) was finally added such that the $[monomer]_0/[Sn]_0$ molar ratio was 283 and the polymerization

was carried out at 100 °C for 7 days and stopped by temperature quenching. A monomer conversion of 92 wt% was determined, yielding grafted-PCL chains with a M_n estimated at ca. 1600 g mol^{-1} based on previously reported data [14,15].

The clay content in the so-produced PCL-grafted CL30B nanohybrid was checked by TGA (Q 50 from TA Instrument, 20 °C/min under helium) giving an inorganic content of 24.7 wt%.

For the sake of comparison, a non-grafted-PCL/CL30B nanocomposite (highly filled, i.e., containing 24.8 wt% inorganics) was also prepared by melt mixing CL30B with CAPA®2402 in a Brabender internal mixer at 175 °C for 10 min. Both highly filled nanohybrid and nanocomposite were considered as masterbatches to be dispersed in CPE. The investigated masterbatches are coded as: CL30B-PCL for the grafted-PCL masterbatch while CL30B/CAPA®2402 for the non-grafted-PCL masterbatch. Each code is further completed by two data in parentheses, the first one indicating the amount of clay (expressed as wt% in inorganics) in the related sample and the second data giving the relative amount of PCL. For example, CPE/CL30B/CAPA®2402 (3;8.4) corresponds to the blend of CPE with the non-grafted-PCL oligomer/montmorillonite masterbatch (physical nanocomposite) that contains 3 wt% of clay (inorganics) and 8.4 wt% of PCL (Mn = 4000 g mol^{-1}).

2.3. Preparation of (nano)composites

CPE/layered silicate composites were prepared by melt blending CPE and the PCL-based masterbatches using a Brabender internal mixer operating at 175 °C for 10 min with a rotation speed of 75 rpm. The collected samples were compression-molded into 3 mm-thick plates for 150 s at 175 °C under a pressure of 150 MPa and then rapidly cooled to room temperature.

The dispersions of the PCL-based masterbatches were carried out to produce nanocomposites containing either 3 wt% or 5 wt% of inorganics and therefore 8.4 and 13.7 wt% of PCL, respectively.

Direct clay dispersion (CPE/CL30B), binary blends (CPE/CAPA®2402) and nanocomposites using masterbatches prepared from non-grafted-PCL oligomers (CPE/CL30B/CAPA®2402) have also been studied for the sake of comparison.

Table 1 shows the various (nano)composites prepared during this study.

2.4. Characterization

The morphology of the (nano)composites has been analyzed by Wide-Angle X-Ray Diffraction (WAXD) and Transmission Electron Microscopy (TEM). WAXD patterns were recorded between 1.65° and 30° (by steps of 0.04°) with a Siemens D5000 diffractometer operating with Cu Kα radiation (λ = 1.5406 Å). TEM micrographs were obtained with a Philips CM100 apparatus using an acceleration voltage of 100 kV. Ultrathin sections (ca. 80 nm thick) were cut at −100 °C from 3 mm thick hot-pressed plates by using a Reichert-Jung Ultracut FC4E microtome equipped with a diamond knife. Because of the large difference in electron density between silicate and polymer matrix, no selective staining was required. TEM analysis has been limited to low magnification (*4500) since sample damage was observed when increasing magnification.

Table 1
Description of the studied materials

(Nano)composites	Compatibiliser	Organoclays
Pristine Tyrin®3611P		
CPE(0;0)	–	–
3 wt% of inorganics and/or 8.4 wt% of PCL		
CPE/CL30B(3;0)	–	CL30B
CPE/CAPA®2402(0;8.4)	CAPA®2402	–
CPE/CL30B/CAPA®2402(3;8.4)	CAPA®2402	CL30B
CPE/CL30B-PCL(3;8.4)	Grafted-PCL	CL30B
5 wt% of inorganics and/or 13.7 wt% of PCL		
CPE/CL30B(5;0)	–	CL30B
CPE/CAPA®2402(0;13.7)	CAPA®2402	–
CPE/CL30B/CAPA®2402(5;13.7)	CAPA®2402	CL30B
CPE/CL30B-PCL(5;13.7)	Grafted-PCL	CL30B

DSC Q100 from TA Instrument was used for Differential Scanning Calorimetry (DSC) analysis. (Nano)composites samples (weighing ≈12 mg) were sealed in aluminum DSC pans and placed in the DSC cell. The DSC was calibrated with indium. Samples were heated from −80 °C to 180 °C with a heating rate of 10 °C/min. DSC analyses were performed with 'fresh' samples, i.e. 48 h after preparation.

Dynamic mechanical thermal analyses (DMTA) were performed with a DMA2980 from TA Instrument from −70 °C to 100 °C on compression molded (0.5-mm thick and 5-mm wide) sheets of either unfilled CPE or CPE/layered silicates nanocomposites. Measurements were carried out in tensile mode at 1 Hz with a deformation amplitude of 20 μm. The heating rate was 3 °C/min.

Tensile tests were performed with a Lloyd LR 10 K tensile testing apparatus. Tensile properties were measured at 20 °C with a constant deformation rate of 50 mm min^{-1} on dumbbell-shaped specimens prepared from compression molded samples according to the 638 type V ASTM norm. Tensile data were evaluated on the average of five independent measurements.

3. Results and discussion

3.1. Materials morphology

3.1.1. Pristine CPE

Tyrin®3611 P, the CPE matrix used in this study, is a commercial formulation including solid additives (such as talc <7 wt%) that may interfere with the characterization of the prepared nanocomposites. Therefore, a morphological study of as-received CPE has been carried out. The WAXD pattern of CPE is presented in Fig. 1. The broad peak at 2θ = 21.2° corresponds to the (110) reflection of polyethylene-type crystalline domains formed by the non-chlorinated fragments of CPE [31]. The diffraction peaks at 2θ = 9.4°, 18.9°, 28.5° correspond to the (001), (002), and (003) reflections of talc [32]. The TEM micrographs (Fig. 2) show the presence of talc particles, which appear as dark objects indicated by white arrows. Due to the

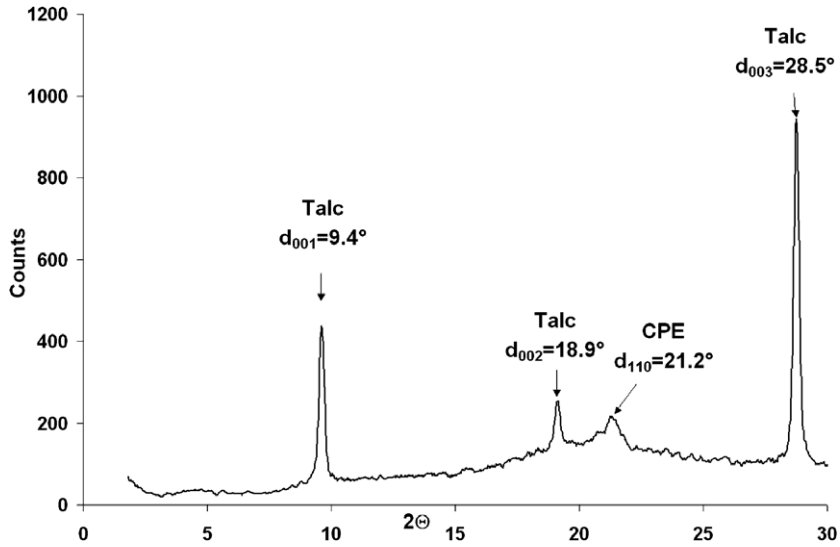

Fig. 1. WAXD pattern for Tyrin® 3611P: CPE and talc characteristic peaks.

strong morphological similarities between clay and talc [33], it will be necessary to take into account the presence of the talc stabilizer for when interpreting the TEM images of the nanocomposites.

3.1.2. (Nano)composites

The WAXD patterns of the CPE (nano)composites with 3 and 5 wt% of clay (the CPE/clay direct blends, and the nanocomposites based on the non-grafted masterbatch and the grafted masterbatch) are presented in Figs. 3 and 5. The diffraction peak of talc at $2\theta = 9.4°$ is clearly visible. The patterns of the CPE/CL30B(3;0) and CPE/CL30B(5;0) direct blends present a diffraction peak at $2\theta = 6.13°$ (interlayer distance $d = 1.43$ nm) characteristic of the CL30B stacks after thermal degradation. Indeed, compared to d_{001} of the starting CL30B detected at 1.84 nm, an interlayer collapse by ca. 0.4 nm is recorded, indicating that melt processing CL30B with a polymer such as CPE at 175 °C for 10 min is mainly due to the double bonds oxidation of tallow alkyl chain ammonium followed by a local cross-linking between long alkyl chain ammoniums, as reported elsewhere [23]. Such decrease of the interlayer spacing also indicates that CPE does not penetrate the clay galleries; the direct blends between CL30B and CPE are microcomposites. In the CPE/CL30B/CAPA®2402(3;8.4) and CPE/CL30B/CAPA®2402(5;13.7) nanocomposites based on the non-grafted masterbatch, the interlayer distance of the organo-clay, calculated from the observed diffraction peaks using the Bragg's equation, is $d = 3.38$ nm ($2\theta = 2.6°$) and $d = 4.06$ nm ($2\theta = 2.34°$), respectively. The increase of the interlayer distance from $d = 1.84$ nm ($2\theta = 4.7°$) in CL30B indicates that polymer intercalation has occurred. It is worth noting that the pre-mixing of the organomodified clay with PCL at 175 °C prior to its dispersion in CPE at 175 °C somehow hinders the degradation of the organo-clay since no diffraction peak around $2\theta = 6°$ is observed. With respect to the nanocomposites with 3 wt% of clay, those with 5 wt% of clay have well-marked diffraction peaks of higher order, meaning that the aggregates have maintained a relatively high level of order. In the CPE/CL30B-PCL(3;8.4) and CPE/CL30B-PCL(5;13.7) nanocomposites based on PCL-grafted masterbatches, the signal corresponding to the interlayer distance of CL30B has broadened considerably, and its maximum is detected at

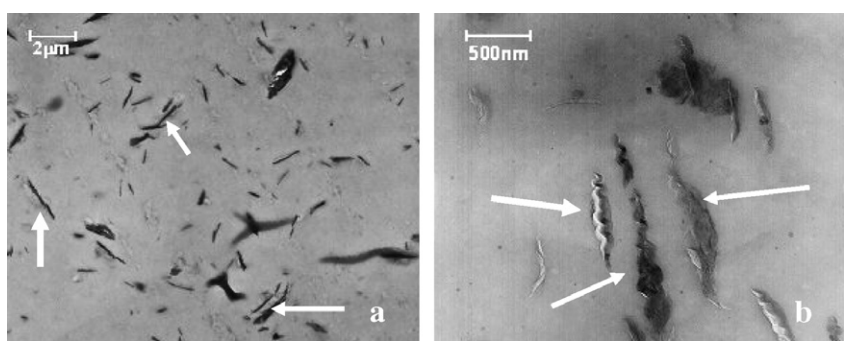

Fig. 2. TEM micrographs for Tyrin® 3611P at low magnification (a), and at high magnification (b). The dark objects on each micrograph represent inorganic particles (talc) contained in the commercial matrix.

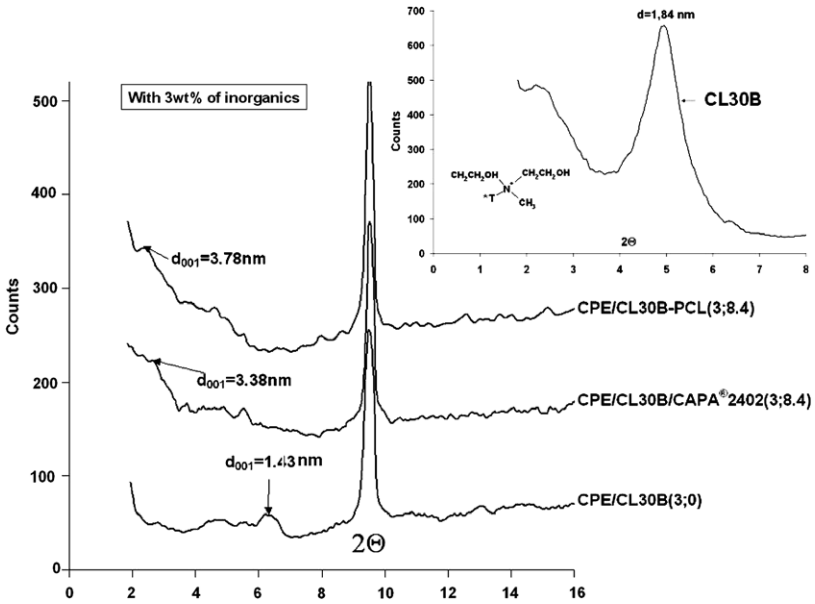

Fig. 3. WAXD patterns for CPE (nano)composites: CPE/CL30B(3;0), CPE/CL30B/CAPA®2402(3;8.4) and CPE/CL30B-PCL(3;8.4).

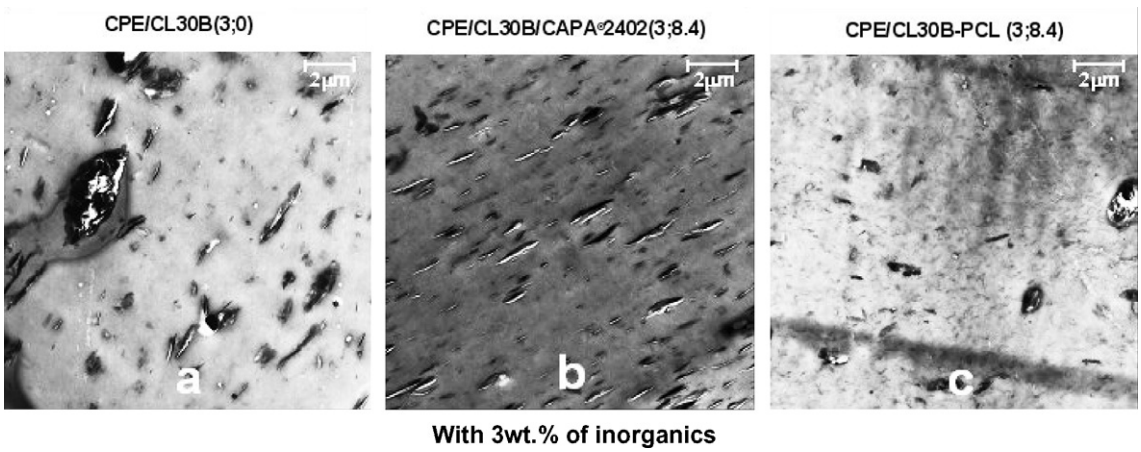

Fig. 4. TEM micrographs for CPE nanocomposites: CPE/CL30B(3;0) (a), CPE/CL30B/CAPA®2402(3;8.4) (b) and CPE/CL30B-PCL(3;8.4) (c).

a higher distance (lower 2θ angle) than in CL30B, i.e., at $d = 3.78$ nm ($2\theta = 2.3°$) and $d = 4.3$ nm ($2\theta = 2.05°$), respectively. Both the broadening of the signal and its shift to lower 2θ angle values are characteristics of more disordered intercalation. The observation of such broad and poorly defined diffraction peaks in the nanocomposites based on grafted masterbatches might also indicate some level of exfoliation, further confirmed by TEM.

Additional information about the morphology of these (nano)composites has been obtained by TEM (see the representative TEM micrographs at low magnification in Figs. 4a and 6). The images confirm a microcomposite structure for the direct blends, without clay nanoplatelet delamination (Figs. 4a and 6a), and an intercalated structure when using a non-grafted masterbatch (Figs. 4b and 6b). For both composites, the talc and clay particles appear as large aggregates of up to a few microns; talc and clay cannot be distinguished at low magnification. The images of the nanocomposites based on the grafted masterbatch (Figs. 4c and 6c) show a semi-intercalated, semi-exfoliated structure with a homogeneous dispersion of exfoliated platelets, together with some small stacks remaining. The large particles that are still visible in the TEM images are talc. These observations will be of key importance for understanding the properties and the effect of clay exfoliation reported hereafter.

3.2. Thermal characterization

3.2.1. (Nano)composites with 8.4 wt% of PCL

The thermal properties of the chlorinated polyethylene composites were studied by DSC (Fig. 7). The thermograms

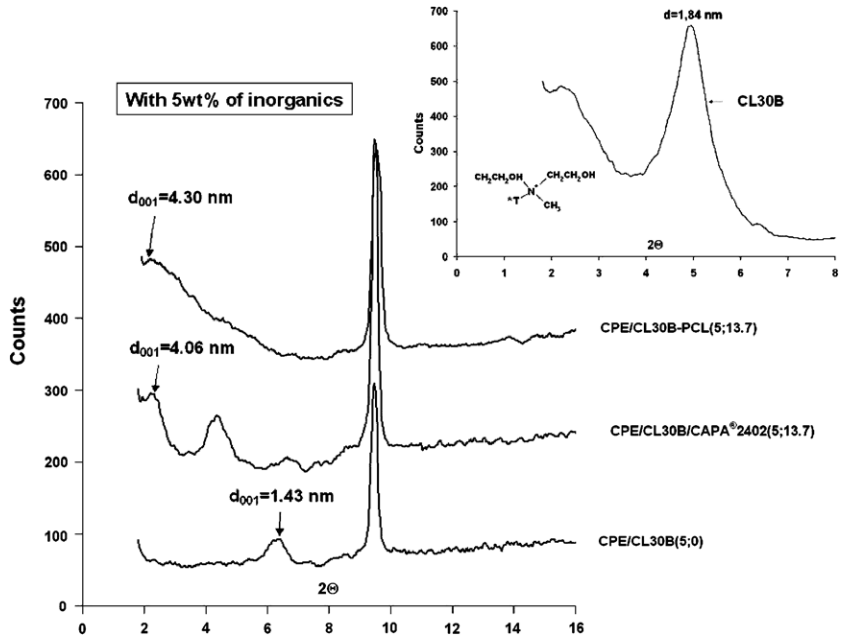

Fig. 5. WAXD patterns for CPE (nano)composites: CPE/CL30B(5;0), CPE/CL30B/CAPA®2402(5;13.7) and CPE/CL30B-PCL(5;13.7).

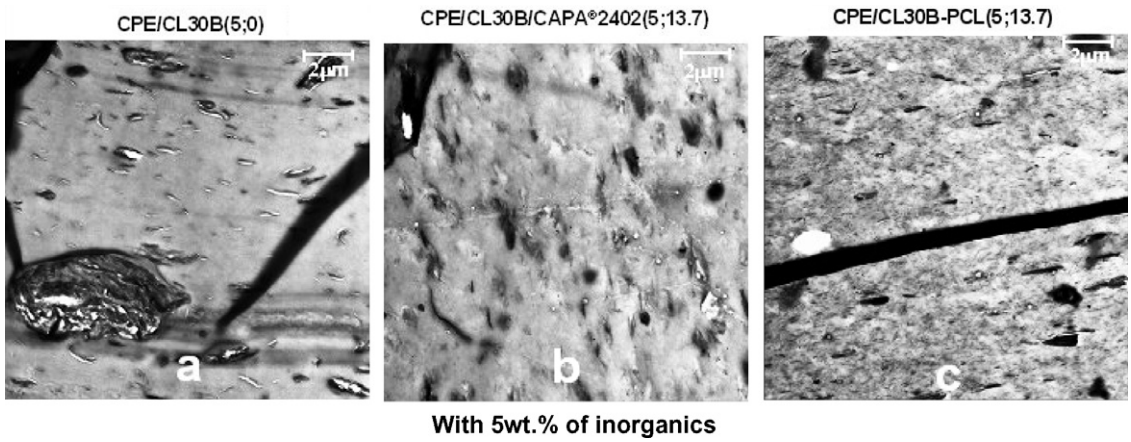

Fig. 6. TEM micrographs for CPE nanocomposites: CPE/CL30B(5;0) (a), CPE/CL30B/CAPA®2402(5;13.7) (b) and CPE/CL30B-PCL(5;13.7) (c).

have been shifted vertically in order to facilitate the interpretation. CPE is characterized by a very broad and complex thermal behavior between −20 °C and 125 °C, comprising both the glass transition and a very broad melting endotherm. In CPE/PCL blends, which can be either totally or partially miscible [25], both phases can crystallize depending on the blend composition. With 8.4 wt% of PCL, no PCL melting peak could be observed neither in the binary blend (CPE/CAPA®2402(0;8.4)) nor in the CPE/CL30B-PCL(3;8.4) nanocomposite. In the nanocomposite based on the non-grafted-PCL masterbatch (CPE/CL30B/CAPA®2402(3;8.4)), an endothermic peak at is however detected ∼50 °C and it's probably corresponds to the melting of some PCL crystalline phase. This might indicate a possible nucleation effect of the organo-modified clay for PCL oligomers when they are not grafted onto the clay surface.

3.2.2. (Nano)composites with 13.7 wt% of PCL

Fig. 8 shows the DSC curves of the CPE (nano)composites and blends containing 13.7 wt% PCL. The observation of the PCL melting peak with a maximum at ca. 52 °C in the first heating scan attests for the presence of some crystalline PCL immiscible with the CPE. The presence of a crystalline PCL phase strongly influences the mechanical properties of the resulting materials, as depicted hereafter.

3.3. DMTA studies

Dynamic mechanical thermal analysis (DMTA) can provide reliable information on the storage modulus of polymer-based materials. The temperature dependence of the storage moduli is presented in Figs. 9–11 for the different (nano)composites.

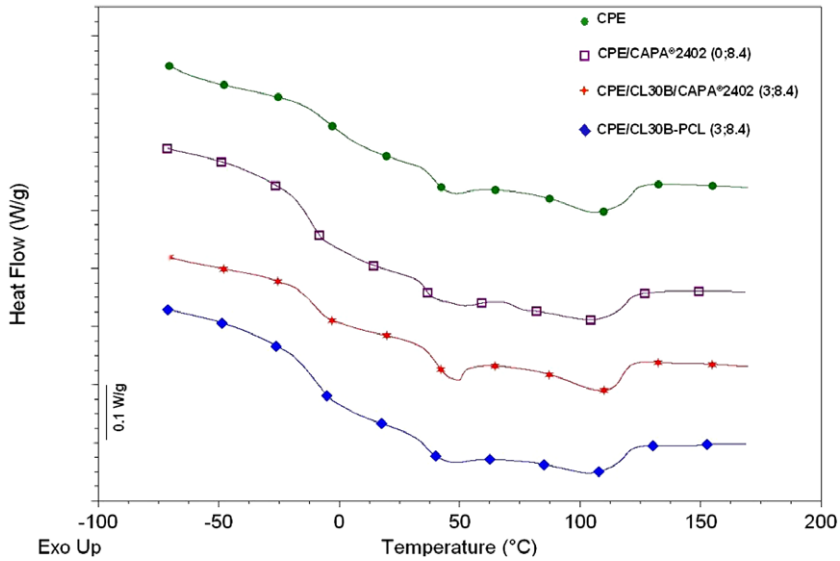

Fig. 7. DSC traces of CPE, CPE/CAPA®2402(0;8.4), CPE/CL30B/CAPA®2402(3;8.4) and CPE/CL30B-PCL(3;8.4) during a first scan at a heating rate of 10 °C/min.

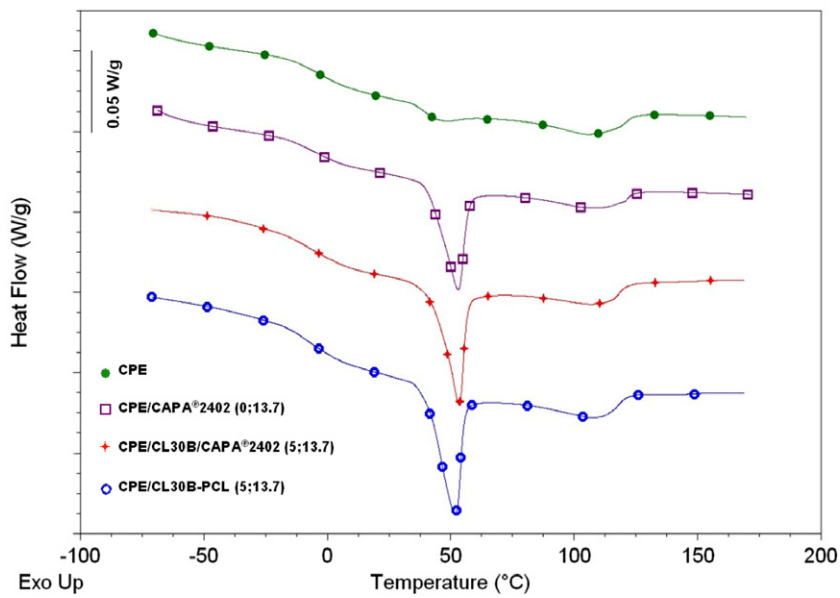

Fig. 8. DSC traces of CPE, CPE/CAPA®2402(0;13.7), CPE/CL30B/CAPA®2402(5;13.7) and CPE/CL30B-PCL(5;13.7) during a first scan at a heating rate of 10 °C/min.

Fig. 9 shows the evolution of the storage modulus (E') with temperature for CPE and CPE/CL30B blends with 3 wt% and 5 wt% of inorganics. E' decreases gradually upon heating from −70 °C with a rapid decrease in the glass transition region of CPE, starting around −10 °C. From 70 °C to 60 °C, E' of the composites is comparable to that of pristine CPE. These results indicate that CL30B has no influence on the CPE mechanical properties in this temperature range, as expected for microcomposites at such low filler contents. However, it is worth pointing out that, at temperatures higher than 60 °C, the presence of clay (3 wt% or 5 wt%) leads to a significant loss in E'. This loss of E' might be associated with modification of the so called α-relaxation process, i.e., the enhanced mobility of some chain segments in CPE (mainly non-chlorinated methylene groups) as a result of lower dipole–dipole interactions in the presence of the clay.

Fig. 10 shows E' for CPE and binary blends with 8.4 and 13.7 wt% of PCL. The storage modulus of the CPE/CAPA®2402(0;8.4) blend observed from −70 °C to 100 °C is lower than that of pristine CPE in the same temperature range. This behavior reflects the plasticizing effect of the

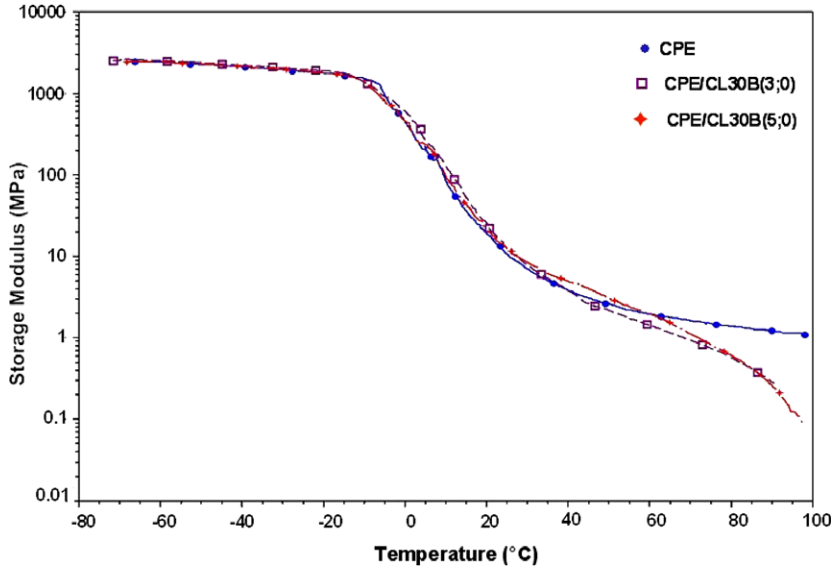

Fig. 9. DMTA traces of CPE, CPE/CL30B(3;0) and CPE/CL30B(5;0).

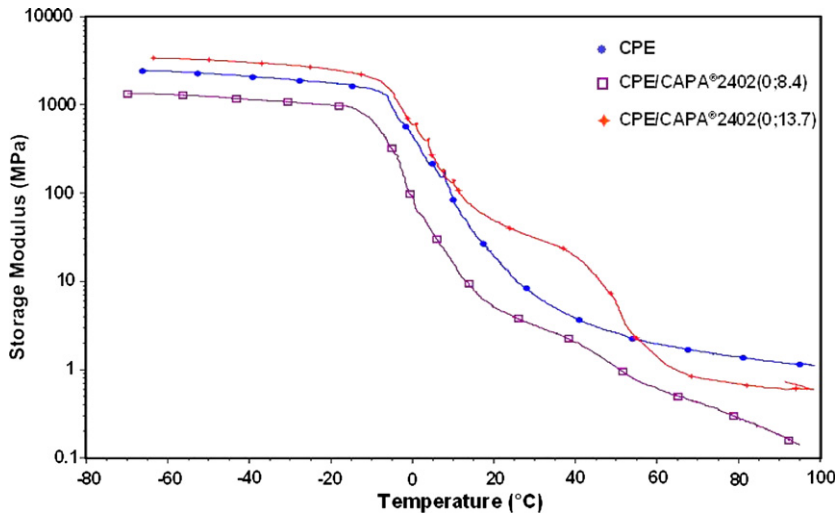

Fig. 10. DMTA traces of CPE, CPE/CAPA®2402 (0;8.4) and CPE/CAPA®2402(0;13.7).

PCL oligomers at this particular weight fraction. On the contrary, the storage modulus of the CPE/CAPA®2402(0;13.7) blend observed in the region from −70 °C to 50 °C, is higher than the E' value recorded for pristine CPE and reflects the increase of the structure stiffness due to the presence of PCL crystallites. At room temperature, E' of CPE/CAPA®2402 (0;13.7) blend shows an increase by ca. 260% in comparison with pristine CPE. At higher temperature, after melting of the PCL crystallites (>50 °C), this blend shows a pronounced drop in storage modulus which becomes lower than that of CPE. This phenomenon can be explained by the plasticization effect of the PCL oligomer or a specific perturbation of the α-relaxation process of CPE by molten PCL chains. The different behavior for PCL-containing blends at temperature higher than 50 °C, as a function of the PCL content, could be explained by a different localization of the PCL chains in the heated blend. For the samples containing 8.4 wt% PCL, this plasticizer is homogenously distributed within the still semi-crystalline CPE, optimizing the plasticizing effect. For the sample containing 13.7 wt% PCL, the melting of the PCL crystalline domains within a still crystalline CPE leads to local increases in the PCL concentration and therefore to a less effective plasticizing effect.

Fig. 11 shows *E'* for CPE, CPE/CL30B-PCL(3;8.4) and CPE/CL30B-PCL(5;13.7) samples. The storage moduli of both CPE nanocomposites are higher than *E'* recorded for the pristine CPE matrix at least from the glassy to the rubbery state. This improvement is directly linked to the fine nanoclay dispersion. One can note the higher storage moduli

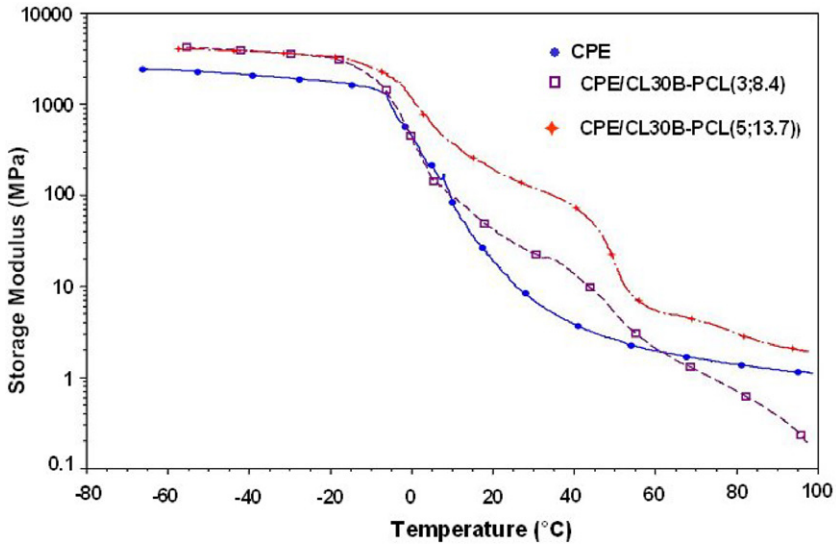

Fig. 11. DMTA traces of CPE, CPE/CL30B-PCL(3;8.4) and CPE/CL30B-PCL(5;13.7).

Table 2
Glass transition temperature of CPE-based materials recorded as the maximum of tan δ in DMTA analysis (20 μm deformation in tensile mode at 1 Hz and 3 °C/min)

Material code	Grafted-PCL	T_g (°C)
CPE (0;0)	–	10.2
CPE/CAPA®2402(0;8.4)	No	0.0
CPE/CAPA®2402(0;13.7)	No	6.5
CPE/CL30B/CAPA®2402(3;8.4)	No	−0.1
CPE/CL30B/CAPA®2402(5;13.7)	No	5.5
CPE/CL30B-PCL(3;8.4)	Yes	3.8
CPE/CL30B-PCL(5;13.7)	Yes	6.1

values for the nanocomposite filled with 5 wt% of inorganics and 13.7 wt% of grafted-PCL chains. Indeed, at 20 °C, a E' value of 193.9 MPa is measured for CPE/CL30B-PCL(5;13.7), which corresponds to an increase by more than 1000%, whereas with 3 wt% of inorganics, the CPE/CL30B-PCL(3;8.4) nanocomposite displays a E' value of 42 MPa, i.e. an increase of 226% (at 20 °C).

The interpretation of these curves have to take into account the combination of several effects such as mechanical reinforcement by exfoliated clay nanoplatelets, partial plasticization by grafted-PCL chains and physical reinforcement by PCL partial crystallization, especially with 13.7 wt% of PCL. In order to shed some light on the plasticization effect of the grafted-PCL chains, values of glass transition temperature (T_g) recorded as the maximum of tan δ for the various studied materials are compared in Table 2. The addition of 8.4 wt% of CAPA®2402 (alone or combined with CL30B, i.e., the physical masterbatch) to the CPE matrix leads to some shift of the T_g value from 10.2 °C down to 0 °C, indicating some miscibility between the two polymers within the amorphous phase. In contrast, the addition of 13.7 wt% of PCL leads to the formation of PCL crystallites that reduce the relative amount of amorphous PCL (cf. Fig. 8). Since only one T_g (at 6.5 °C for the binary blend and at 5.5 °C for the nanocomposite filled with the non-grafted-PCL-based masterbatch) is still observed, one can infer a good miscibility of the CPE and PCL amorphous phases but expectedly the fraction of miscible PCL is highly reduced.

For the sample based on 8.4 wt% of PCL-grafted at the surface of the layered silicates (CPE/CL30B-PCL(3;8.4)), a T_g of 3.8 °C is recorded, without any PCL melting peak (cf. Fig. 7). This T_g higher than the value corresponding to the related binary blend (0 °C) can be interpreted by a lower of PCL weight fraction available for mixing within the CPE amorphous phase, due to the PCL tethering onto the organo-clay layers. A still higher T_g value (6.1 °C) is found for samples based on 13.7 wt% of grafted-PCL (CPE/CL30B-PCL(5;13.7)), which can be correlated to the presence of a melting endotherm in DSC for these materials (see Fig. 8), indicating the formation of PCL crystallites and thus a lower available amount of amorphous polyester chains. To conclude, partial plasticization occurs in each blend but is less pronounced when 1°) PCL is grafted onto the clay and 2°) PCL partially crystallizes, i.e. in presence of with 13.7 wt% PCL.

Therefore, Fig. 11 allows determining three regimes of mechanical improvement, depending on both the temperature and the presence of PCL crystalline domains:

- From −70 °C to −5 °C, the higher storage moduli for the nanocomposites are essentially due to the large extent of clay exfoliation. At this stage, the assessment of the antagonist effects arising from PCL plasticization and PCL crystallite reinforcement proved highly difficult.
- From −5 to 60 °C, a reinforcing effect arising from the presence of PCL crystallites in the 5 wt%-nanofilled samples can clearly been observed, especially in the 10 to 40 °C range, where the E' values of the nanocomposites can reach more than 20 times the value recorded for the pristine CPE. Moreover, even if such an enhancement of the storage modulus is also observed for the binary

CPE/PCL blends (Fig. 10), a fivefold increase in E' is found for the composition containing 13.7 wt% of PCL with respect to pristine CPE. Such a behavior clearly indicates a positive effect of the exfoliated nanoparticles on E' within this temperature range.

- From 60 to 100 °C, PCL being in the molten state, the mechanical reinforcement is essentially insured by the presence of exfoliated clay layers. The large drop in E' for the nanocomposite with 3 wt% of clay may be due to a significant influence of the PCL-grafted nanoclay, at low concentration, on the α-relaxation process of CPE matrix [34] while a particularly strong reinforcing effect is observed for the nanocomposite filled with 5 wt% of PCL-grafted clay.

Fig. 12, which compares the temperature evolution of the storage modulus for the various samples containing 13.7 wt% of PCL, i.e. the binary CPE/CAPA®2402(0;13.7) blend, the nanocomposites based on non-grafted-PCL CPE/CL30B/CAPA®2402(5;13.7) and grafted-PCL CPE/CL30B-PCL(5;13.7), further confirms this synergistic effect between clay exfoliation and PCL partial crystallization. Below CPE glass transition, the storage moduli of CPE/CAPA®2402(0;13.7) and CPE non-grafted-PCL nanocomposite are comparable whereas E′ of grafted-PCL nanocomposites is slightly higher, due to clay exfoliation. Above CPE glass transition, the storage modulus of non-grafted-PCL nanocomposite appears higher than E' of pristine CPE, however it remains lower than E' of the grafted-PCL nanocomposite. Indeed, for example at 20 °C, the storage modulus of CPE/CL30B/CAPA®2402(5;13.7) is measured at 83.1 MPa (a 447% increase with respect to pristine CPE) whereas for CPE/CL30B-PCL(5;13.7), the storage modulus increases by 1043%. In all cases, E' tends to decrease drastically after the PCL melting (>50 °C) but exfoliated PCL-grafted nanocomposites preserve a much higher storage modulus compared to the other two materials, further confirming the large influence of clay nanoplatelets exfoliation.

To summarize, the dispersion in CPE of a nanohybrid masterbatch prepared by controlled grafting polymerization to reach 5 wt% of inorganics allows to improve drastically the stiffness of CPE nanocomposites, especially in the 10 °C to 40 °C range of temperature. This improvement is due to a synergistic effect of nanoclay exfoliation and PCL partial crystallization.

In order to shed some light on the possible mechanisms responsible for such a large stiffness improvement in CPE/CL30B-PCL(5;13.7), the relative storage moduli (ratio of the CPE-based materials storage modulus to the CPE matrix storage modulus) E'_{rel} for binary, non-grafted and grafted-PCL blends with 13.7 wt% of PCL have been calculated and are displayed vs. temperature in Fig. 13. Clearly, E'_{rel} values higher than 1 indicate stiffness reinforcement of CPE while values below 1 typically indicate some plasticization effect. Four different zones can be distinguished depending on the temperature. Below the CPE glass transition (zone A), the relative storage modulus of CPE/CL30B-PCL(5;13.7) is higher than both CPE/CAPA®2402(0;13.7) and CPE/CL30B/ CAPA®2402(5;13.7) blends, reflecting the effect on modulus of the fine clay nanoplatelets dispersion (high degree of exfoliation). In zone A, all the samples display values higher than 1, indicating also some mechanical reinforcement by the presence of PCL crystallites. Zone B corresponds to the beginning of the glass transition of the materials, i.e., activation of large molecular motions in the amorphous part of the materials. In this temperature zone, the CPE/Cl30B-PCL(5;13.7) nanocomposite distinctly shows a higher relative storage modulus in comparison with the other two materials. However, it is in the zone C (from 10 °C to 60 °C) that the evolution of the relative storage moduli with temperature shows tremendous differences between the three samples. In this temperature range, the sample experiences various thermal transitions associated with the two polymeric components of the blend, i.e., the second half of the CPE glass transition, melting of PCL crystallites, the endothermic transition (relaxa-

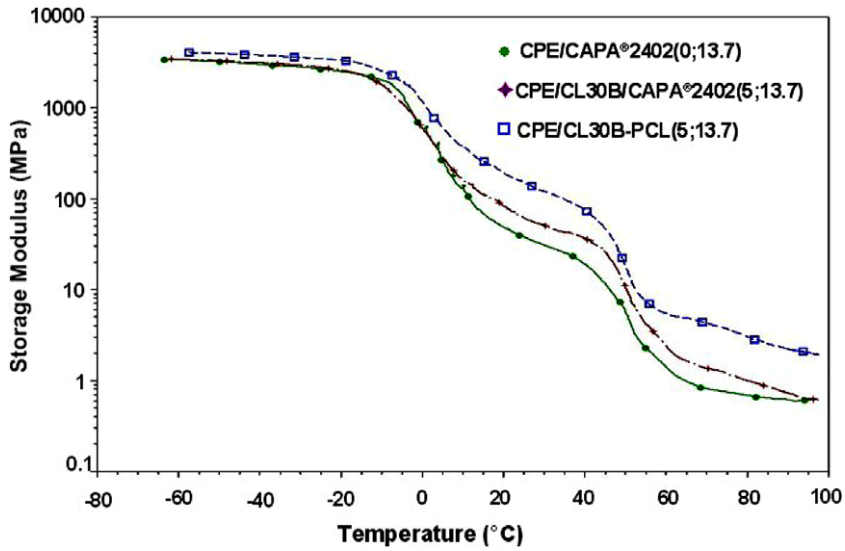

Fig. 12. DMTA traces of CPE/CAPA®2402(0;13.7), CPE/CL30B/CAPA®2402(5;13.7) and CPE/CL30B-PCL(5;13.7).

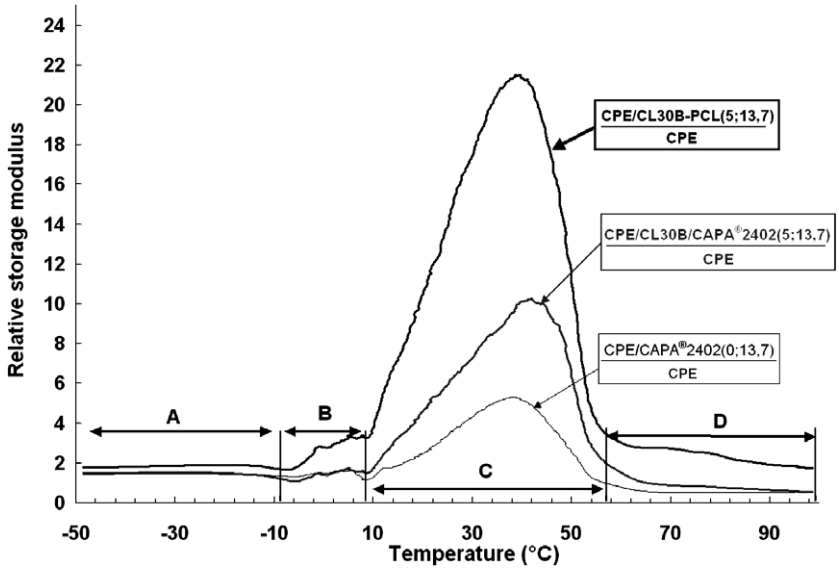

Fig. 13. Temperature dependence of the relative storage modulus (with respect to the CPE matrix) for CPE/CAPA®2402(0;13.7), CPE/CL30B/CAPA®2402(5;13.7), and CPE/CL30B-PCL(5;13.7).

tion or melting) of the CPE matrix (see Fig. 8). The CPE/CAPA®2402(0;13.7) binary blend shows a moderate increase of its relative storage modulus (up to 5.4 at 38 °C) followed by a rapid decrease to E'_{rel} lower than 1. This decrease is clearly related to the melting of the PCL crystallites. To understand the reason for the former increase in E'_{rel}, it is necessary to observe how E' of the binary blend deviates from E' of CPE (Fig. 10). Clearly, E'_{rel} increases because the binary blend maintains some stiffness while CPE experiences a fast decrease of E'. Since this increase disappears with the melting of PCL crystallites, it is therefore their presence that is responsible for the relative storage modulus increase for the binary blend. In the binary blend, PCL crystallites really act as reinforcing nano-objects dispersed in the CPE matrix. The same phenomenon (i.e., an increase of E'_{rel}) prevails for the largely exfoliated CPE/CL30B-PCL(5;13.7) nanocomposite but the increase in E'_{rel} is much more important and reaches a value of 21.8 at 38 °C. Such a high increase cannot be explained only by the presence of PCL crystallites and highly dispersed nanoclays. For the mostly intercalated CPE/CL30B/CAPA®2402(5;13.7) nanocomposite, an intermediate increase of E'_{rel} (with a maximum of 10.4 at 41 °C) is measured.

This large variation in storage modulus, clearly related to the presence of PCL crystallites, could result from the formation of some kind of supramolecular network within the CPE matrix built from the interconnection of nanometric clay platelets and PCL crystallites. This network would largely reinforce the CPE matrix until melting of the PCL crystallites. The characterization of this supramolecular organization is under current investigation by atomic force microscopy techniques and will be presented in a forthcoming paper.

Finally above the melting of PCL crystallites (zone D), CPE/CAPA®2402(0;13.7) and CPE/CL30B/CAPA®2402(5;13.7) exhibit E'_{rel} values lower than 1, indicating plasticization of CPE by the molten PCL in these materials. The intercalated nanocomposite however displays E'_{rel} values slightly superior to the binary blend, due to the presence of the intercalated and probably scarcely exfoliated clay. The exfoliated CPE/CL30-PCL(5;13.7) nanocomposite is characterized by E'_{rel} values in the D zone higher than 1 due to the reinforcing effect of the delaminated clay nanoplatelets.

3.4. Mechanical Properties of (nano)composites

In order to evaluate the macroscopic effect of CPE/layered silicate–PCL nanohybrid preparation, tensile tests have also been performed. The results are reported in Fig. 14. CPE is a ductile polymer able to sustain large deformations (1130% for elongation at break) and characterized by a relatively low Young's modulus of 8.6 ± 0.4 MPa. When dispersing CL30B directly in CPE, a Young's modulus of 6.7 ± 1.3 MPa is measured for the sample with 3 wt% of inorganics while 11.3 ± 0.7 MPa is measured at 5 wt% of inorganics. The ultimate properties remain comparable to pristine CPE. So the direct addition of organo-modified clay does not significantly improve the mechanical properties of CPE. This can mainly be linked to the poor clay dispersion. The binary blend with 8.4 wt% of PCL is characterized by a decrease of Young's modulus down to 2.4 ± 0.7 MPa and an increase of elongation at break up to 1343 ± 48%. These results attest for the plasticization effect operated by the introduction of the PCL. In contrast, the binary blend with 13.7 wt% of PCL is characterized by a Young's modulus increased up to 22.9 ± 0.8 MPa and a significant decrease of elongation at break down to 769 ± 170% which can be linked to the presence of PCL crystallites acting as rigid fillers. The nanocomposite with non-grafted-PCL clay masterbatch at 5 wt% of inorganics is characterized by a higher modulus at 33.3 ± 1.7 MPa and an elongation at

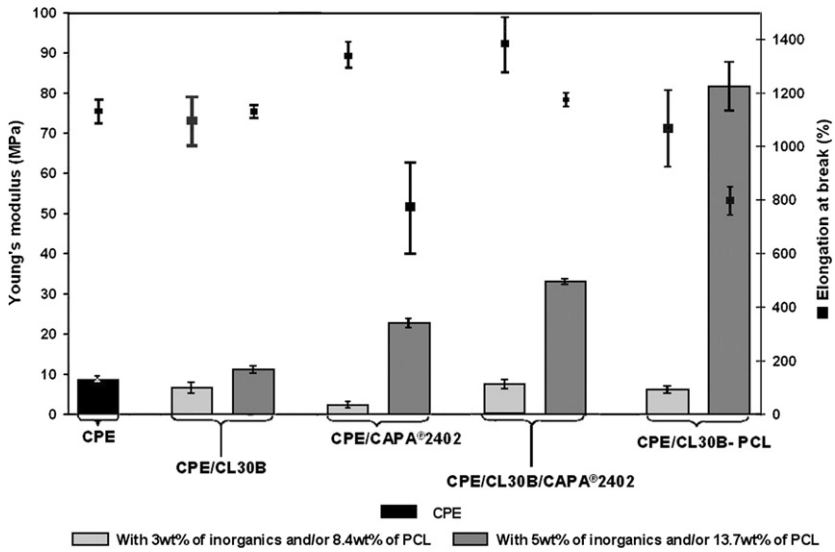

Fig. 14. Young's modulus (bar graphs) and elongation at break (black squares) for CPE, CPE/CL30B, CPE/CAPA®2402, CPE/CL30B/CAPA®2402 and CPE/CL30B-PCL with 3 wt% of inorganics and/or 8.4 wt% of PCL and with 5 wt% of inorganics and/or 13.7 wt% of PCL.

break comparable to pristine CPE (1179 ± 25%). This reinforcement is already remarkable and confirms the interest of the use of clay at 5 wt% of inorganics and 13.7 wt% of partially crystallized PCL.

The nanocomposites prepared from grafted-PCL-clay masterbatches present a different behavior. At 3 wt% of inorganics (8.4 wt% of grafted-PCL), the CPE/CL30B-PCL(3;8.4) nanocomposite shows a Young's modulus and ultimate properties comparable to the direct blend in spite of a good dispersion. This phenomenon can be explained by the two antagonist effects of PCL plasticization and the exfoliated clay reinforcement, as previously discussed.

The most interesting results are, however, obtained with the nanocomposites containing 5 wt% of inorganics and 13.7 wt% of grafted-PCL. Indeed, the Young's modulus is measured at 81.6 ± 6 MPa for CPE/CL30B-PCL(5;13.7), so a 950% increase compared to pristine CPE, with still acceptable ultimate properties for such a materials (796 ± 53% of elongation at break).

4. Conclusions

Largely exfoliated CPE/layered silicate nanocomposites have been prepared using PCL-grafted organo-clay nanohybrids as masterbatches to promote extensive clay delamination. The highly filled nanohybrids are obtained in a first step by controlled ring-opening intercalative polymerization of ε-caprolactone from hydroxyl-bearing ammonium cations organo-modifying the clay. Then, the PCL-grafted organo-clay nanohybrids are added as masterbatches in CPE by melt blending. This two-step preparation of nanocomposites leads to largely exfoliated morphologies with 3 wt% or 5 wt% of inorganics.

At room temperature, tensile properties of the resulting nanocomposites are drastically enhanced when the two following conditions are encountered:

- A good dispersion of the individual clay layers promoted by grafted-PCL chains;
- A sufficiently high amount of grafted-PCL chains to promote partial PCL crystallization within the CPE matrix.

Clearly, a synergistic effect in mechanical reinforcement of CPE has been evidenced through the partial crystallization of grafted-PCL chains tethered to the surface of the delaminated nanoplatelets, which might form a supramolecular network of interconnected clay platelets and PCL crystallites. Interestingly, this PCL-grafted masterbatch strategy can be implemented in other polymer matrices since PCL has shown to be miscible with a large variety of polymer matrices.

Acknowledgements

The authors wish to thank Prof. A. Rulmont (General Chemistry and Physical Chemistry Department, University of Liège) for the WAXD analyses. S. Benali and P. Brocorens are grateful to "Région Wallonne" for a Grant in the frame of the WINNOMAT program: PROCOMO. UMH and Materia Nova asbl are grateful for the financial support from the 'Région Wallonne' and the European Commission (FSE, FEDER) in the frame of Objectif-1 and Phasing-Out programs. This work was partially supported by the Belgian Federal Science Policy Office (PAI6/27) and by the Belgian National Fund for Scientific Research (FRS-FNRS).

References

[1] Alexandre M, Dubois Ph. Polymer-layered silicate nanocomposite: preparation, properties and uses of a new class of materials. Mater Sci Eng R 2000;28:1–63.
[2] Giannelis EP. Polymer layered silicate nanocomposites. Adv Mater 1996;8:29–35.
[3] Biswas M, Sinha Ray S. Recent progress in synthesis and evaluation of polymer–montmorillonite nanocomposites. Adv Polym Sci 2001;155:167–221.

[4] Tjong SC. Structural and mechanical properties of polymer nanocomposites. Mater Sci Eng R 2006;53:73–197.
[5] Gilman JW. Flammability and thermal stability studies of polymer layered-silicate (clay) nanocomposites. Appl Clay Sci 1999;15:31–49.
[6] Gorrasi G, Tortora M, Vittoria V, Pollet E, Lepoittevin B, Alexandre M, et al. Vapor barrier properties of polycaprolactone montmorillonite nanocomposites: effect of a clay dispersion. Polymer 2003;44:2271–9.
[7] Yano K, Usuki A, Okada A. Synthesis and properties of polyimide-clay hybrid films. J Polym Sci Part A: Polym Chem 1997;35:2289–94.
[8] Komori Y, Kuroda K. Polymer-clay nanocomposites. In: Pinnavaia TJ, Beall GW, editors. NewYork: John Wiley and Sons Ltd.; 2001. p. 3–18.
[9] Heinemann J, Reichert P, Thomann R, Mülhaupt R. Polyolefin nanocomposites formed by melt compounding and transition metal catalyzed ethene homo- and copolymerization in the presence of layered silicates. Macromol Rapid Commun 1999;20:423–30.
[10] Gopakumar TG, Lee JA, Kontopoulou M, Parent JS. Influence of clay exfoliation on the physical properties of montmorillonite/polyethylene composites. Polymer 2002;43:5483–91.
[11] Zhang Q, Wang Y, Fu Q. Shear-induced change of exfoliation and orientation in polypropylene/montmorillonite nanocomposites. J Polym Sci Part B: Polym Phys 2002;41:1–10.
[12] Chiu FC, Lai SM, Chen JW, Chu PH. Combined effects of clay modifications and compatibilizers on the formation and physical properties of melt-mixed polypropylene/clay nanocomposites. J Polym Sci Part B: Polym Phys 2004;42:4139–50.
[13] Ke Y, Long C, Qi Z. Crystallization, properties, and crystal and nanoscale morphology of PET-clay nanocomposites. J Appl Polym Sci 1999;71:1139–46.
[14] Lepoittevin B, Pantoustier N, Devalckenaere M, Alexandre M, Kubies D, Calberg C, et al. Pol(ε-caprolactone)/clay nanocomposites prepared by melt intercalation: mechanical, thermal, and rheological properties. Macromolecules 2002;35:8385–90.
[15] Lepoittevin B, Pantoustier N, Alexandre M, Calberg C, Jérôme R, Dubois Ph. Polyester layered silicate nanohybrids by controlled grafting polymerization. J Mater Chem 2002;12:3528–32.
[16] Hu X, Lesser AJ. Effect of a silicate filler on the crystal morphology of poly(trimethylene terephthalate)/clay nanocomposites. J Polym Sci 2003;41:2275–89.
[17] Lepoittevin B, Pantoustier N, Devalckenaere M, Alexandre M, Calberg C, Jérôme R, et al. Polymer/layered silicate nanocomposites by combined intercalative polymerization and melt intercalation: a masterbatch process. Polymer 2003;44:2033–40.
[18] March J, editor. Advanced organic chemistry reactions mechanisms and structures. New York: Mc Graw J. Hill; 1977. p. 631–40.
[19] Marchand GR, editor. Polymeric materials encyclopedia. CRC Press; 1996. p. 1234–8.
[20] Abu-Isa IA. Degradation of chlorinated polyethylene-III: effect of additives on dehydrochlorination and oxygen absorption. Polym Eng Sci 1975;15:299–307.
[21] Young WL, Rouge B, Posey B, Process for the chlorination of polyolefins, U.S. Patent 3 454 544, patented July 8, 1969.
[22] Kim Y, White JL. Melt-Intercalation nanocomposites with chlorinated polymers. J Appl Polym Sci 2003;90:1581–8.
[23] Benali S, Peeterbroeck S, Larrieu J, Laffineur F, Pireaux JJ, Alexandre M, et al. Study of interlayer spacing collapse during polymer/clay nanocomposite melt intercalation. J Nanosci Nanotechnol 2008;8:1707–13.
[24] Fornes TD, Yoon PJ, Paul DR. Polymer matrix degradation color formation in melt processed nylon 6/clay nanocomposites. Polymer 2003;44:7545–56.
[25] Shah RK, Paul DR. Nylon 6 nanocomposites prepared by a melt mixing masterbatch process. Polymer 2004;45:2991–3000.
[26] Ren J, Huang Y, Liu Y, Tang X. Preparation, characterization and properties of poly(vinyl chloride)/compatibilizer/organophilic-montmorillonite nanocomposites by melt intercalation. Polym Test 2005;24:316–23.
[27] Defieuw G, Groeninckx G, Reynaers H. Miscibility and morphology of binary polymer blends of polycaprolactone with solution-chlorinated polyethylene. Polymer 1989;30:595–603.
[28] Messersmith PB, Giannelis EP. Synthesis and barrier properties of poly(ε-caprolactone)-layered silicate nanocomposites. J Polym Sci, Part A: Polym Chem 1995;33:1047–57.
[29] Panstoustier N, Lepoittevin B, Alexandre M, Kubies D, Calberg C, Jérôme R, et al. Biodegradable polyester layered silicate nanocomposites based on poly(ε-caprolactone). Polym Eng Sci 2002;42:1928–37.
[30] Kubies D, Panstoustier N, Dubois Ph, Jérôme R. Controlled ring-opening polymerization of ε-caprolactone in the presence of layered silicates and formation of nanocomposites. Macromolecules 2002;35:3318–20.
[31] Stoeva S, Popov A, Rodriguez R. Wide angle X-ray diffraction study of the solid-phase chlorinated poly(ethylene). Polymer 2004;45:6341–8.
[32] Ferrage E, Martin F, Petit S, Pejo-Soucaille S, Micoud P, Fourty G, et al. Evaluation of talc morphology using FTIR and H/D substitution. Clay Minerals 2003;38:141–50.
[33] Yalcin B, Cakmak M. The role of plasticizer on the exfoliation and dispersion and fracture behavior of clay particles in PVC matrix: a comprehensive morphological study. Polymer 2004;45:6623–38.
[34] Perena JM, Fatou JG, Guzman J. Dynamic mechanical behaviour of chlorinated polyethylene. Makromol Chem 1980;181:1349–56.